Received: 30 November 2021 | Revised: 13 February 2022 | Accepted: 17 February 2022

IET Quantum Communication

DOI: 10.1049/qtc2.12036

The Institution of Engineering and Technology WILEY

ORIGINAL RESEARCH

Performance of coherent-state quantum target detection in the context of asymmetric hypothesis testing

Gaetana Spedalieri | **Stefano Pirandola**

Department of Computer Science, University of York, York, North Yorkshire, UK

Correspondence

Stefano Pirandola, Department of Computer Science, University of York, York, North Yorkshire, YO10 5GH, UK.
Email: Stefano.pirandola@york.ac.uk

Funding information

European Union's Horizon 2020 Research and Innovation Action, Grant/Award Number: grant agreement No. 862644

Abstract

Due to the difficulties of implementing joint measurements, quantum illumination schemes that are based on signal-idler entanglement are difficult to implement in practice. For this reason, one may consider quantum-inspired designs of quantum lidar/radar where the input sources are semi-classical (coherent states) while retaining the quantum aspects of the detection. The performance of these designs could be studied in the context of asymmetric hypothesis testing by resorting to the quantum Stein's lemma. However, here the authors discuss that, for typical finite-size regimes, the second- and third-order expansions associated with this approach are not sufficient to prove quantum advantage.

KEYWORDS

quantum information, quantum theory

1 | INTRODUCTION

In coherent-state quantum target detection, one employs a semi-classical source, specifically coherent states but a quantum detection scheme, not necessarily homodyne or heterodyne detection (which are used classically [1]). This can therefore be considered a quantum-inspired radar (QIR) since we relax the quantum properties of the transmitter (i.e., no use of entanglement, differently from quantum illumination [2–8]) while retaining the optimal quantum performance of the receiver. We assume the single-bin setting that corresponds to looking at some fixed range R and solving a binary test of target absent (null hypothesis H_0) or present (alternative hypothesis H_1). In particular, we perform our study in the setting of asymmetric hypothesis testing [9–17], so that we fix the false-alarm probability to some reasonably low value, for example, $p_{\text{FA}} = 10^{-3}$, and then we minimise the probability of mis-detection p_{MD}. Thus, we look at the performance in terms of mis-detection probability p_{MD} versus the signal-to-noise ratio (SNR) γ.

More precisely, the hypotheses mentioned above correspond to the following:

$\mathbf{H}_0$: A completely thermalising channel, that is, a channel with zero transmissivity in an environment with $\overline{n}_B$ mean thermal photons (target absent).
$\mathbf{H}_1$: A lossy channel with transmissivity η and thermal noise $\overline{n}_B/(1-\eta)$, where the re-scaling avoids the possibility of a passive signature (target present).

Let us consider an input coherent state $|\alpha\rangle$ with a mean number of photons $\overline{n}_S = |\alpha|^2$ and a mean value $\overline{\mathbf{x}}_S = (\overline{q}, \overline{p})^T = \sqrt{2}(\text{Re}\alpha, \text{Im}\alpha)^T$. Without losing generality, we can assume that α is real, so that $\overline{\mathbf{x}}_S = (\overline{q}, \overline{p})^T = \sqrt{2}(\alpha, 0)^T$. On reflection from the potential target, we have two possible output states:

$\mathbf{H}_0$: A thermal state ρ_0^{th} with zero mean $\overline{\mathbf{x}}_0 = 0$ and the covariance matrix (CM) $\mathbf{V}_0 = (\overline{n}_B + 1/2)\mathbf{I}$.
$\mathbf{H}_1$: A displaced thermal state ρ_1^{th} with the mean value $\overline{\mathbf{x}}_1 = \sqrt{\eta}\overline{\mathbf{x}}_S$ and same CM $\mathbf{V}_1 = (\overline{n}_B + 1/2)\mathbf{I}$.

Note that we have $\rho_1^{\text{th}} = D(\sqrt{\eta}\,\alpha)\rho_0^{\text{th}}D(-\sqrt{\eta}\,\alpha)$ where D is the phase-space displacement operator.

2 | QIR PERFORMANCE

In the setting of asymmetric hypothesis testing, the maximum performance achievable by a QIR is given by the quantum Stein's lemma [9, 10, 13, 15]. Suppose we want to discriminate between M copies of two states, ρ_0 and ρ_1, using an optimal quantum measurement with output $k = 0, 1$. At fixed false-alarm probability $p_{\rm FA} := p\left(1|\rho_0^{\otimes M}\right)$, we have the following decay of the false-negative (mis-detection) probability

$$p_{\rm MD} := p\left(0|\rho_1^{\otimes M}\right) \simeq \exp(-\beta M), \tag{1}$$

for some rate or error exponent β. According to the quantum Stein's lemma, the optimal rate β is equal to the relative entropy between the two states, that is,

$$\beta = D(\rho_0\|\rho_1) := \mathrm{Tr}[\rho_0(\ln\rho_0 - \ln\rho_1)]. \tag{2}$$

In a more refined version, we account for second-order asymptotics in M and write Ref. [18] (see also Refs [15, 17])

$$p_{\rm MD} = e^{-MD(\rho_0\|\rho_1) - \sqrt{MV(\rho_0\|\rho_1)}\Phi^{-1}(p_{\rm FA}) + \mathcal{O}(\log M)}, \tag{3}$$

where we also use the quantum relative entropy variance

$$V(\rho_0\|\rho_1) = \mathrm{Tr}\left[\rho_0(\ln\rho_0 - \ln\rho_1)^2\right] - [D(\rho_0\|\rho_1)]^2, \tag{4}$$

and the cumulative distribution function

$$\Phi(\varepsilon) := \frac{1}{\sqrt{2\pi}}\int_{-\infty}^{\varepsilon} dx\, \exp\left(-x^2/2\right), \tag{5}$$

with $\varepsilon \in (0, 1)$ corresponding to (or bounding) the false-alarm probability $p_{\rm FA}$.

However, we need to notice that the term $\mathcal{O}(\log M)$ in Equation (3) may play a non-trivial role in SNR calculations where M is not so large. According to Theorem 5 of Ref. [18], we have that $\mathcal{O}(\log M)$ is between 0 and 2 log M, so that we have upper and lower bounds for $p_{\rm MD}$ (with quite some gap). A more refined calculation involves to compute the third moment T appearing in that theorem. This will give more refined upper and lower bounds for the performance of coherent states.

3 | FIRST- AND SECOND-ORDER TERMS

We can write explicit formulae for the relative entropy $D(\rho_0\|\rho_1)$ and the relative entropy variance $V(\rho_0\|\rho_1)$ of two arbitrary N-mode Gaussian states, $\rho_0(\bar{\mathbf{x}}_0, \mathbf{V}_0)$ and $\rho_1(\bar{\mathbf{x}}_1, \mathbf{V}_1)$. The first one is given by Ref. [19]

$$D(\rho_0\|\rho_1) = -\Sigma(\mathbf{V}_0, \mathbf{V}_0) + \Sigma(\mathbf{V}_0, \mathbf{V}_1), \tag{6}$$

where we have defined the function

$$\Sigma(\mathbf{V}_0, \mathbf{V}_1) = \frac{\ln\det\left(\mathbf{V}_1 + \frac{i\boldsymbol{\Omega}}{2}\right) + \mathrm{Tr}\left(\mathbf{V}_0\mathbf{G}_1\right) + \delta^T\mathbf{G}_1\delta}{2}, \tag{7}$$

with $\delta = \bar{\mathbf{x}}_0 - \bar{\mathbf{x}}_1$ and $\mathbf{G}_k = 2i\boldsymbol{\Omega}\coth^{-1}(2i\mathbf{V}_k\boldsymbol{\Omega})$ being the Gibbs matrix for CM $\mathbf{V}_k$ (with $k = 0, 1$) [20]. The second one is given by Ref. [21, 22]

$$V(\rho_0\|\rho_1) = \frac{\mathrm{Tr}\left[(\boldsymbol{\Gamma}\mathbf{V}_0)^2\right]}{2} + \frac{\mathrm{Tr}\left[(\boldsymbol{\Gamma}\boldsymbol{\Omega})^2\right]}{8} + \delta^T\mathbf{G}_1\mathbf{V}_0\mathbf{G}_1\delta, \tag{8}$$

where $\boldsymbol{\Gamma} = \mathbf{G}_0 - \mathbf{G}_1$. Using the output states, $\rho_0^{\rm th}$ and $\rho_1^{\rm th}$, it is easy to compute

$$D := D\left(\rho_0^{\rm th}\|\rho_1^{\rm th}\right) = \eta\bar{n}_S\ln\left(1 + \bar{n}_B^{-1}\right) = \gamma\bar{n}_B\ln\left(1 + \bar{n}_B^{-1}\right), \tag{9}$$

$$\begin{aligned} V &:= V\left(\rho_0^{\rm th}\|\rho_1^{\rm th}\right) = \eta\bar{n}_S\left(2\bar{n}_B + 1\right)\ln^2\left(1 + \bar{n}_B^{-1}\right) \\ &= \gamma\bar{n}_B\left(2\bar{n}_B + 1\right)\ln^2\left(1 + \bar{n}_B^{-1}\right), \end{aligned} \tag{10}$$

where $\gamma := \eta\bar{n}_S/\bar{n}_B$ is the SNR. Note that, for large background noise $\bar{n}_B \gg 1$, we can expand

$$D \simeq \gamma + \mathcal{O}\left(\bar{n}_B^{-1}\right),\ V \simeq 2\gamma + \mathcal{O}\left(\bar{n}_B^{-2}\right). \tag{11}$$

Following Ref [18, Theorem 5], we may write the following (approximate) bounds

$$\frac{\Lambda}{M^2} \lesssim p_{\rm MD} \lesssim \Lambda, \tag{12}$$

where

$$\Lambda := \exp\left[-MD - \sqrt{MV}\,\Phi^{-1}(p_{\rm FA})\right]. \tag{13}$$

The upper bound in Equation (12) is the tool typically used in the literature, while the lower bound is not taken into account (despite the fact that the gap between the two bounds can become quite large).

4 | COMPUTATION OF THE THIRD-ORDER MOMENT

A more accurate version of Equation (12) includes higher-order terms and suitable conditions of validity. Following Ref [18], let us introduce the third-order (absolute) moment

$$T(\rho_0\|\rho_1) = \sum_{x,y}\left|\langle a_x|b_y\rangle\right|^2\alpha_x\left|\ln\frac{\alpha_x}{\beta_y} - D(\rho_0\|\rho_1)\right|^3, \tag{14}$$

where, we use the spectral decompositions of the states

$$\rho_0 = \sum_x \alpha_x |a_x\rangle\langle a_x|, \ \rho_1 = \sum_y \beta_y |b_y\rangle\langle b_y|. \tag{15}$$

See Appendix A for more details about the notation behind the formula in Equation (14).

Let $0 < C < 0.4748$ be the constant in the Berry–Esseen theorem [23, 24]. Then, we may write the more accurate bounds Ref. [18, Theorem 5]

$$\begin{aligned} &\frac{1}{2^9 M^2}\exp\left[-MD(\rho_0\|\rho_1) - \sqrt{MV(\rho_0\|\rho_1)}\,\Phi^{-1}(\theta_L)\right] \\ &\qquad \le p_{\mathrm{MD}} \le \\ &\exp\left[-MD(\rho_0\|\rho_1) - \sqrt{MV(\rho_0\|\rho_1)}\,\Phi^{-1}(\theta_U)\right], \end{aligned} \tag{16}$$

where

$$\theta_L := p_{\mathrm{FA}} + \frac{1}{\sqrt{M}}\left(\frac{CT}{V(\rho_0\|\rho_1)^{3/2}} + 2\right), \tag{17}$$

$$\theta_U := p_{\mathrm{FA}} - \frac{1}{\sqrt{M}}\frac{CT}{V(\rho_0\|\rho_1)^{3/2}}. \tag{18}$$

More precisely, the bounds in Equation (16) are valid as long as M is large enough to guarantee that $\theta_L \le 1$ and $\theta_U \ge 0$, so that they fall in the domain of Φ^{-1}. From Equation (16), we can again notice how the lower bound become loose for increasing M.

Let us compute the third moment T for the output states ρ_0^{th} and ρ_1^{th}, associated with the two hypotheses (see Introduction). We have the following number-state spectral decompositions.

$$\rho_0^{\mathrm{th}} = \sum_{k=0}^{\infty} \gamma_k |k\rangle\langle k|, \quad \gamma_k := \frac{\overline{n}_B^k}{\left(\overline{n}_B + 1\right)^{k+1}}, \tag{19}$$

$$\begin{aligned} \rho_1^{\mathrm{th}} &= D(\sqrt{\eta}\,\alpha)\rho_0^{\mathrm{th}} D(-\sqrt{\eta}\,\alpha) \\ &= \sum_{k=0}^{\infty} \gamma_k |k, \sqrt{\eta}\,\alpha\rangle\langle k, \sqrt{\eta}\,\alpha|, \end{aligned} \tag{20}$$

where $|k, \sqrt{\eta}\,\alpha\rangle = D(\sqrt{\eta}\,\alpha)|k\rangle$ is a displaced number state.

Using these decompositions in Equation (14), we find

$$\begin{aligned} T\left(\rho_0^{\mathrm{th}}\|\rho_1^{\mathrm{th}}\right) &= \sum_{k,l=0}^{\infty} |\langle k|l, \sqrt{\eta}\,\alpha\rangle^2 \gamma_k \left|\ln\tfrac{\gamma_k}{\gamma_l} - D(\rho_0\|\rho_1)\right|^3 \\ &= \sum_{k,l=0}^{\infty} \left|\langle k|D(\sqrt{\eta}\ \alpha)|l\rangle\right|^2 \gamma_k \left|\ln\tfrac{\gamma_k}{\gamma_l} - D(\rho_0\|\rho_1)\right|^3. \end{aligned} \tag{21}$$

Because

$$D\left(\rho_0^{\mathrm{th}}\|\rho_1^{\mathrm{th}}\right) = \eta\overline{n}_S \ln\left(\frac{\overline{n}_B + 1}{\overline{n}_B}\right), \tag{22}$$

$$\frac{\gamma_k}{\gamma_l} = \frac{\overline{n}_B^{k-l}}{\left(\overline{n}_B + 1\right)^{k-l}}, \tag{23}$$

$$\ln\frac{\gamma_k}{\gamma_l} = (k-l)\ln\left(\frac{\overline{n}_B}{\overline{n}_B + 1}\right), \tag{24}$$

we may simplify

$$\begin{aligned} T\left(\rho_0^{\mathrm{th}}\|\rho_1^{\mathrm{th}}\right) &= \sum_{k,l=0}^{\infty} \left|\langle k|D(\sqrt{\eta}\ \alpha)|l\rangle\right|^2 \\ &\quad \times \gamma_k \left|(k - l + \eta\overline{n}_S)\ln\left(\tfrac{\overline{n}_B}{\overline{n}_B+1}\right)\right|^3. \end{aligned} \tag{25}$$

Now recall that [25, Eq. (3.30) and Appendix B]

$$\langle k|D(\alpha)|l\rangle = \sqrt{\frac{l!}{k!}}\alpha^{k-l}e^{-|\alpha|^2/2}\mathcal{L}_l^{(k-l)}\left(|\alpha|^2\right), \tag{26}$$

where $\mathcal{L}_n^{(m)}(x)$ is an associated Laguerre polynomial, which takes the following form in terms of the binomial coefficient [26]

$$\mathcal{L}_n^{(m)}(x) := \sum_{k=0}^{n}\binom{n+m}{n-k}\frac{(-x)^k}{k!}. \tag{27}$$

Therefore, for $\overline{n}_S = |\alpha|^2$, we may compute

$$\left|\langle k|D(\sqrt{\eta}\ \alpha)|l\rangle\right|^2 = \frac{l!}{k!}(\eta\overline{n}_S)^{k-l}e^{-\eta\overline{n}_S}\left[\mathcal{L}_l^{(k-l)}\left(\eta\overline{n}_S\right)\right]^2, \tag{28}$$

so that we find the analytical expression

$$\begin{aligned} T\left(\rho_0^{\mathrm{th}}\|\rho_1^{\mathrm{th}}\right) &= e^{-\eta\overline{n}_S}\sum_{k,l=0}^{\infty}\frac{l!}{k!}\gamma_k(\eta\overline{n}_S)^{k-l}\left[\mathcal{L}_l^{(k-l)}\left(\eta\overline{n}_S\right)\right]^2 \\ &\quad \times \left|(k - l + \eta\overline{n}_S)\ln\left(\frac{\overline{n}_B}{\overline{n}_B+1}\right)\right|^3. \end{aligned} \tag{29}$$

Note that this expression can be put in terms of the SNR $\gamma = \eta\overline{n}_S/\overline{n}_B$ and the thermal background $\overline{n}_B$, that is, we may equivalently write

$$\begin{aligned} T\left(\rho_0^{\mathrm{th}}\|\rho_1^{\mathrm{th}}\right) &= e^{-\gamma\overline{n}_B}\sum_{k,l=0}^{\infty}\frac{l!}{k!}\gamma_k(\gamma\overline{n}_B)^{k-l}\left[\mathcal{L}_l^{k-l}(\gamma\overline{n}_B)\right]^2 \\ &\quad \times \left|(k - l + \gamma\overline{n}_B)\ln\left(\frac{\overline{n}_B}{\overline{n}_B+1}\right)\right|^3. \end{aligned} \tag{30}$$

Furthermore, suitable bounds might be used for the Laguerre polynomials (see Appendix B).

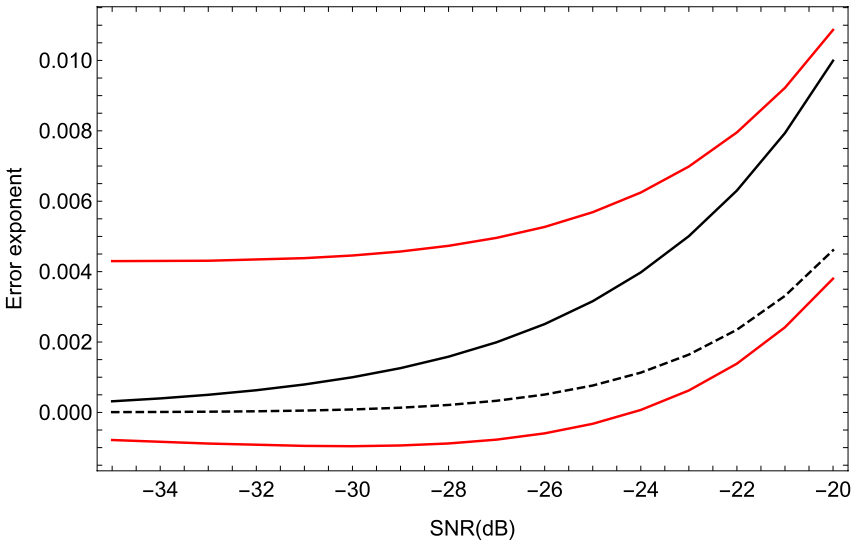

FIGURE 1 Error exponent $\varepsilon_{\mathrm{MD}}$ as a function of the signal-to-noise ratio in dBs $10\log_{10}\gamma$. We compare the first order approximation of Equation (1) (black line), with the higher-order lower and upper bounds from Equation (16) (red lines). We also plot the Marcum benchmark (dashed black line). We consider the parameters $p_{\mathrm{FA}} = 10^{-3}$, $M = 5000$ and $\overline{n}_B = 600$. Note that the lower bound even becomes negative for lower values of SNRs

5 | NUMERICAL INVESTIGATION

In order to perform a numerical comparison, we consider the error exponent

$$\varepsilon_{\mathrm{MD}} := \frac{-\ln p_{\mathrm{MD}}}{M}, \tag{31}$$

that corresponds to β in Equation (1) at the first order. It is clear that the higher the value of $\varepsilon_{\mathrm{MD}}$ is, the better is the discrimination performance.

To show the finite-size behaviour, we consider $p_{\mathrm{FA}} = 10^{-3}$, $M = 5000$ and bright background $\overline{n}_B = 600$. With these parameters, we plot $\varepsilon_{\mathrm{MD}}$ versus SNR in decibels (i.e., $10\log_{10}\gamma$) for the optimised detection of coherent states considering the first order formula of Equation (1) and the higher-order bounds in Equation (16). As a comparison, we also plot the error exponent achievable by a classical radar, which employs coherent state pulses and heterodyne detection [1]. This can be computed from the Marcum Q-function [27, 28]

$$p_{\mathrm{MD}} = 1 - Q\left(\sqrt{2\gamma}, \sqrt{-2\ln p_{\mathrm{FA}}}\right), \tag{32}$$

$$Q(x,y) := \int_y^\infty dt\ te^{-(t^2+x^2)/2} I_0(tx), \tag{33}$$

with $I_0(.)$ being the modified Bessel function of the first kind of zero order.

As we can see from Figure 1, the QIR would have a clear advantage over the Marcum benchmark if we consider the asymptotic first order formula. However, the first order expression of Equation (1) is valid only for very large M. For a typical finite size value of M, we need to consider the higher-order bounds in Equation (16), but we see that the gap is too large to reach a conclusion of quantum advantage.

6 | CONCLUSION

In this work, we have studied a quantum-inspired lidar/radar based on coherent states and optimal quantum detection, analysing the performance in the context of asymmetric hypothesis testing (quantum Stein's lemma, higher-order asymptotics). According to our study, the current mathematical tools do not allow us to prove quantum advantage over classical strategies based on coherent states and heterodyne detection when a finite number of probes is considered. Such an advantage may be claimed in the asymptotic limit of a very large number of probes, so that the first order becomes completely dominant over the higher-order terms. However, such an asymptotic regime is not relevant for practical applications.

ACKNOWLEDGEMENTS

This work has been funded by the European Union's Horizon 2020 Research and Innovation Action under grant agreement No. 862644 (FET Open project: Quantum readout techniques and technologies, QUARTET). Stefano Pirandola would like to thank Quntao Zhuang for discussions.

CONFLICT OF INTEREST

The authors declare no conflict of interest.

DATA AVAILABILITY STATEMENT

Data and code related to the findings of this manuscript can be found at https://github.com/softquanta/QIR.

ORCID

Stefano Pirandola https://orcid.org/0000-0001-6165-5615

REFERENCES

1. Merrill, I.S., et al.: Introduction to Radar Systems. McGraw-Hill, New York (1981)
2. Lloyd, S.: Enhanced sensitivity of photodetection via quantum illumination. Science 321, 1463–1465 (2008)

3. Pirandola, S., Lloyd, S.: Computable bounds for the discrimination of Gaussian states. Phys. Rev. A. 78(1), 012331 (2008)
4. Tan, S.-H., et al.: Quantum illumination with Gaussian states. Phys. Rev. Lett. 101, 253601 (2008)
5. Barzanjeh, S., et al.: Microwave quantum illumination. Phys. Rev. Lett. 114(8), 080503 (2015)
6. Zhuang, Q., Zhang, Z., Shapiro, J.H.: Entanglement-enhanced lidars for simultaneous range and velocity measurements. Phys. Rev. A. 96, 040304 (2017)
7. Zhuang, Q., Zhang, Z., Shapiro, J.H.: Quantum illumination for enhanced detection of Rayleigh-fading targets. Phys. Rev. A. 96, (R), 020302 (2017)
8. Pirandola, S., et al.: Advances in photonic quantum sensing. Nat. Photon. 12, 724–733 (2018)
9. Hiai, F., Petz, D.: The proper formula for relative entropy and its asymptotics in quantum probability. Commun. Math. Phys. 143, 99–114 (1991)
10. Hayashi, M.: Asymptotics of quantum relative entropy from a representation theoretical viewpoint. J. Phys. A. Math. Gen. 34, 3413–3419 (2001)
11. Hayashi, M.: Optimal sequence of quantum measurements in the sense of Stein's lemma in quantum hypothesis testing. J. Phys. A. Math. Gen. 35, 10759–10773 (2002)
12. Hayashi, M.: Two quantum analogues of Fisher information from a large deviation viewpoint of quantum estimation. J. Phys. A. Math. Gen. 35, 7689–7727 (2002)
13. Ogawa, T., Nagaoka, H.: Strong Converse and Stein's Lemma in Quantum Hypothesis Testing, Asymptotic Theory Of Quantum Statistical Inference: Selected Papers, pp. 28-42. World Scientific, Singapore (2005)
14. Audenaert, K.M.R., et al.: Asymptotic error rates in quantum hypothesis testing. Commun. Math. Phys. 279, 251–283 (2008)
15. Tomamichel, M., Hayashi, M.: A hierarchy of information quantities for finite block length Analysis of quantum tasks. IEEE Trans. Inf. Theor. 59, 7693–7710 (2013)
16. Spedalieri, G., Braunstein, S.L.: Asymmetric quantum hypothesis testing with Gaussian states. Phys. Rev. A. 90, 052307 (2014)
17. Zhuang, Q., Zhang, Z., Shapiro, J.H.: Entanglement-enhanced Neyman–Pearson target detection using quantum illumination. J. Opt. Soc. Am. B 34, 1567–1572 (2017)
18. Li, K.: Second-order asymptotics for quantum hypothesis testing. Ann. Stat. 42, 171–189 (2014)
19. Pirandola, S., et al.: Fundamental limits of repeaterless quantum communications. Nat. Commun. 8, 15043 (2017). See also arXiv:1510.08863 (2015)
20. Banchi, L., Braunstein, S.L., Pirandola, S.: Quantum fidelity for arbitrary Gaussian states. Phys. Rev. Lett. 115, 260501 (2015)
21. Pirandola, S., et al.: Advances in quantum cryptography. Adv. Opt Photon 12, 1012–1236 (2020)
22. Wilde, M.M., et al.: Gaussian hypothesis testing and quantum illumination. Phys. Rev. Lett. 119, 120501 (2017)
23. Korolev, V.Y., Shevtsova, I.G.: On the upper bound for the absolute constant in the Berry-Esseen inequality. Theor. Probab. Appl. 54, 638–658 (2010)
24. Shevtsova, I.: On the absolute constants in the Berry-Esseen type inequalities for identically distributed summands (2011). arXiv:1111.6554
25. Cahill, K.E., Glauber, R.J.: Ordered expansions in boson amplitude operators. Phys. Rev. 177, 1857–1881 (1969)
26. Szegö, G.: Orthogonal Polynomials, vol. 23, 4th ed. Amer. Math. Soc. Colloq. Publ.Amer. Math. Soc., Providence, RI (1975)
27. Marcum, J.I.: A statistical theory of target detection by pulsed radar: mathematical appendix, RAND Corporation, Santa Monica, CA, Research memorandum RM-753. Reprinted in IRE Transactions on Information Theory **IT-6**, 59–267 July 1, 1948 (1960)
28. Albersheim, W.: A closed-form approximation to Robertson's detection characteristics. Proc. IEEE 69, 839 (1981)
29. Nussbaum, M., Szkola, A.: The Chernoff lower bound for symmetric quantum hypothesis testing. Ann. Stat. 37, 1040–1057 (2009)
30. Rooney, P.G.: Further inequalities for generalized Laguerre polynomials. C.R. Math. Rep. Acad. Sci. Can. 7, 273–275 (1985)

How to cite this article: Spedalieri, G., Pirandola, S.: Performance of coherent-state quantum target detection in the context of asymmetric hypothesis testing. IET Quant. Comm. 3(2), 112–117 (2022). https://doi.org/10.1049/qtc2.12036

APPENDIX A

RELATIVE ENTROPY NOTATION [29]

Relative entropy is given by

$$D(\rho_0\|\rho_1) := \mathrm{Tr}[\rho_0(\ln\rho_0 - \ln\rho_1)]. \tag{A1}$$

Using the spectral decompositions

$$\rho_0 = \sum_x \alpha_x |a_x\rangle\langle a_x|,\ \rho_1 = \sum_y \beta_y |b_y\rangle\langle b_y|, \tag{A2}$$

and therefore

$$\ln\rho_0 = \sum_x \ln\alpha_x |a_x\rangle\langle a_x|, \tag{A3}$$

$$\ln\rho_1 = \sum_y \ln\beta_y |b_y\rangle\langle b_y|, \tag{A4}$$

we may write

$$D(\rho_0\|\rho_1) = \sum_x \alpha_x \langle a_x|(\ln\rho_0 - \ln\rho_1)|a_x\rangle \tag{A5}$$

$$= \sum_x \alpha_x \left[\ln\alpha_x - \sum_y \ln\beta_y |\langle a_x|b_y\rangle|^2\right]. \tag{A6}$$

Let us set $|a_x\rangle = \sum_y \gamma_{xy}|b_y\rangle$ with complex γ_{xy} such that $\sum_x |\gamma_{xy}|^2 = \sum_y |\gamma_{xy}|^2 = 1$. Therefore,

$$\begin{aligned} D(\rho_0\|\rho_1) &= \sum_x \alpha_x \left(\ln\alpha_x - \sum_y \ln\beta_y |\gamma_{xy}|^2\right) \\ &= \sum_{x,y} \alpha_x |\gamma_{xy}|^2 \left(\ln\alpha_x - \ln\beta_y\right) \\ &= \sum_{x,y} p_{xy} \ln\frac{\alpha_x}{\beta_y} := \left\langle \ln\frac{\alpha(X)}{\beta(Y)}\right\rangle, \end{aligned} \tag{A7}$$

where $\alpha(X) := \{\alpha_x, p_x\}$, and $\beta(Y) := \{\beta_y, p_y\}$ where p_x and p_y are the marginal distributions of the joint probability $p_{xy} := \alpha_x |\gamma_{xy}|^2$, which is the probability to get $X = x$ and $Y = y$ by measuring ρ_0 in the basis $\{|a_x\rangle\}$ and then in $\{|b_y\rangle\}$. In this notation, we may also write the relative entropy variance as follows:

$$V(\rho_0\|\rho_1) = \left\langle \ln\frac{\alpha(X)}{\beta(Y)}\right\rangle^2 - D(\rho_0\|\rho_1)^2. \tag{A8}$$

The third-order moment entering the quantum Stein's lemma is given by [18]

$$T(\rho_0\|\rho_1) = \left\langle \left|\ln\frac{\alpha(X)}{\beta(Y)} - D(\rho_0\|\rho_1)\right|^3 \right\rangle \tag{A9}$$

$$= \sum_{x,y} |\langle a_x|b_y\rangle|^2 \alpha_x \left|\ln\frac{\alpha_x}{\beta_y} - D(\rho_0\|\rho_1)\right|^3. \tag{A10}$$

APPENDIX B

USEFUL BOUNDS

Various bounds are known for the associated Laguerre polynomials. A well-known uniform bound is the Szegö bound [26]

$$\left|\mathcal{L}_n^{(m)}(x)\right| \le \frac{(m+1)_n}{n!} e^{x/2}, \tag{B1}$$

for $x,\ m \ge 0,\ n = 0, 1, \ldots$where we use the Pochhammer's symbol (or shifted factorial)

$$(a)_0 = 1, \tag{B2}$$

$$(a)_n = a(a+1)(a+2)\cdots(a+n-1), \tag{B3}$$

$$(a)_n = \frac{\Gamma(a+n)}{\Gamma(a)} \tag{B4}$$

with $\Gamma(a)$ being the Gamma function. Another one is Ref. [30]

$$\left|\mathcal{L}_n^{(m)}(x)\right| \le 2^{-m} q_n e^{x/2}, \tag{B5}$$

for $x \ge 0,\ m \le -1/2,\ n = 0, 1, \ldots$ and where we set

$$q_n = \frac{\sqrt{(2n)!}}{2^{n+1/2} n!} \simeq \frac{1}{\sqrt[4]{4\pi n}} \text{ for large } n. \tag{B6}$$